J|A|C|S COMMUNICATIONS

Published on Web 07/02/2009

Three-Dimensional Biomimetic Mineralization of Dense Hydrogel Templates

Gao Liu,*,† Dacheng Zhao,† Antoni P. Tomsia,‡ Andrew M. Minor,‡,§,⊥ Xiangyun Song,† and Eduardo Saiz‡

Environmental Energy Technologies Division, Materials Sciences Division, and National Center for Electron Microscopy, Lawrence Berkeley National Laboratory, Berkeley, California 94720 and Department of Materials Science and Engineering, University of California Berkeley, Berkeley, California 94720

Received May 18, 2009; E-mail: gliu@lbl.gov

In biological materials, form and function are intimately related. From nacre to bone, nature achieves unique structural and functional properties through the combination of organic and inorganic phases in complex hierarchical structures.[1] These natural composites are often created through carefully orchestrated biomineralization processes that result in an extremely accurate control of the shape, size, and distribution of the inorganic crystals.[2] Recreating natural mineralization in the laboratory to build new bioinspired composites is a very attractive prospect but has been extremely difficult.[3−5] This is largely due to the limitations in our basic knowledge of biomineralization and to the technical difficulties associated with ion transport and control of mineral nucleation, growth, and stroichiometry in dense and nanoporous matrices.[2,4] As a result, most mineralization approaches are confined to the manipulation of crystal formation and growth in two dimensions.[3,6]

In this work we describe a technique for three-dimensional mineralization of dense hydrogel scaffolds (Supporting Information, Figure S-1) with an apatitic calcium phosphate mineral whose structure is closely related to the inorganic component of bone. Dense hydrogels are very appealing materials for the synthesis of mineralized, bone-like structures. Natural hydrogels, such as collagen, are the structural scaffolds in various connective tissues including bone, and it is possible to formulate synthetic hydrogels with similar elasticity and water retention ability.[7] Hydrogels can be easily assembled in three dimensions while displaying multiple functional domains, and their polymerization chemistry allows the incorporation of polar ligands that mimic the acidic matrix proteins regulating mineral growth.[8] In nature, microscopic vesicles often act as vehicles for ion transport and provide the microenvironment needed to promote controlled mineral nucleation and assembly. It is believed that matrix vesicles released by the osteoblast plasma membrane play an important role in the mineralization of the extracellular matrix and the formation of bone.[2] In this work, phase separation is used to create liquid vesicles inside a dense hydrogel matrix formulated to provide specific sites for the attachment of Ca ions and template the crystallization of nanoapatite. The ultimate goal is to form a bone-like composite that could be used for the engineering and regeneration of calcified tissue. Because the experimental conditions can be easily controlled, the process can help to clarify some poorly understood aspects in the crystallization of apatite and the origins of the transition between amorphous and crystalline inorganic phases during bone formation.

Promoting ion transport into the organic matrix is one of the key issues in the mineralization of dense polymer networks. Often, this is done through immersion in simulated body fluid or a similar solution.[9−11] As a result, mineralization is slow and difficult to control. In addition, the process works better in a highly porous material with micrometer size pores that facilitate liquid infiltration or in a "soft" polymer with very large equilibrium water contents.[12,13] Here we use a direct electric-current-assisted diffusion approach to promote the transport of Ca^{2+}, PO_4^{3-}, HPO_4^{2-}, and OH^- ions into a dense hydrogel matrix (Figure 1a).[14] Two chambers, one containing a $CaCl_2$ aqueous solution with a Tris-HCl buffer solution (pH = 8) and a positive electrode and the other with a Na_2HPO_4 aqueous solution (pH = 10) and a negative electrode, are connected through the hydrogel. A voltage drop maintains a constant current between the electrodes such that the Ca^{2+} ions migrate toward the negative electrode, while the HPO_4^{2-} and PO_4^{3-} ions move toward the positive one. The only pathway for the ions is through the hydrogel, and they meet at the reaction front inside the organic matrix. By controlling the pH of both electrode chambers, it is possible to promote the precipitation of calcium phosphate mineral when the two counterions meet. Compared to concentration or gravitational diffusion, this current-assisted approach allows careful control over the mineral concentration and precipitation rates, as ion transport can be easily adjusted by changing the current density. As a result it is possible to form previously unattainable mineral morphologies at much higher ion concentrations.

Following nature's approach, the control of ion transport should be combined with the right organic matrix to template mineral

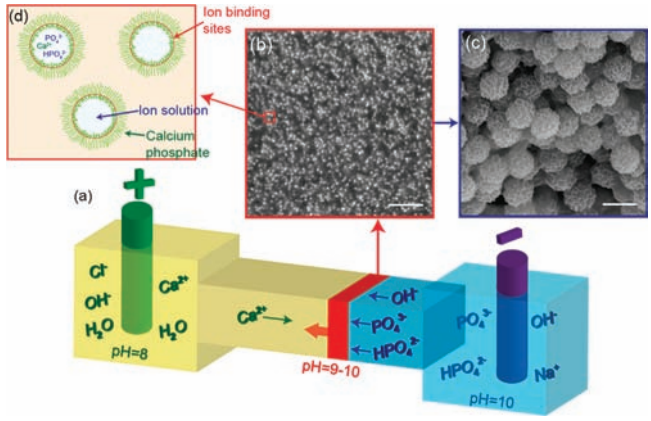

Figure 1. Schematic of the direct current-assisted ion diffusion process. (a) An electrical current is established, and the ions travel through the hydrogel to meet at the reaction front. (b) In situ SEM analysis of a fully hydrated hydrogel. (c) The interconnected spherical mineral domains are clearly visible after removing the organic matrix using a plasma etching treatment. (d) The amide groups in polyacrylamide hydrogel interact with the Ca ions in the solution. The interface between the aqueous domain and the gel acts as a center for the nucleation of an apatitic calcium phosphate mineral (Scale bars: (b) 10 μm; (c) 2 μm).

† Environmental Energy Technologies Division, Lawrence Berkeley National Laboratory.
‡ Materials Sciences Division, Lawrence Berkeley National Laboratory.
§ National Center for Electron Microscopy, Lawrence Berkeley National Laboratory.
⊥ University of California at Berkeley.

formation. It has been shown that synthetic biocompatible hydrogels such as polyacrylamide and polyhydroxyethylmethacrylate (pHEMA) provide a versatile template for the surface mineralization of calcium phosphate films.[15] In our current-assisted diffusion setup, the use of pure pHEMA hydrogels at all concentrations tested resulted in the nucleation of dicalcium phosphate dihydrate (Brushite, DCPD, $CaHPO_4 \cdot 2H_2O$) crystals that precipitate inside the hydrogel and grow into micrometer-sized particles. These particles push away the pHEMA network as they grow (Supporting Information, Figure S-2). Incorporating a few percent of sodium methacrylate into the pHEMA structure significantly alters the morphology of the mineral phase eventually limiting its growth (Supporting Information, Figure S-3) due to the strong interaction of the carboxyl with the calcium ions.

Organic−inorganic integration at the nanoscale was achieved using a polyacrylamide hydrogel due to the strong interaction between the amide groups and the Ca ions.[16] Scanning Electron Microscopy (SEM) shows a structure formed by microspherical mineral aggregates distributed regularly in the organic network (Figure 1b, c). Figure 1b is an "in situ" SEM image of a fully hydrated sample obtained through an electron transparent window, whereas Figure 1c is an image of a dried and plasma etched sample. In Figure 1b, the top portion of these microspheres (white dots) is captured in the image as the sample surface is pressed against the electron transparent window. By comparison the full surface structure of the microsphere is visible in Figure 1c. These results demonstrate that the microspheres are formed during the current-assisted ion diffusion process rather than after drying the hydrogel. The TEM analysis of the micro- and nanostructure of the aggregates (Figure 2) shows that the microspheres are hollow; their size is very uniform and changes inversely with the hydrogel concentration. Mineral nanofibers (5−20 nm wide, 200 nm long) can be observed growing from the surface of these spheres into the hydrogel, while short and broader lamellar nanoparticles (up to 50 nm wide) grow toward the interior. The fibers and lamellae are formed by the assembly of amorphous and crystalline nanodomains (5−20 nm in size). The crystal lattice parameter based on electron diffraction agrees with a semicrystalline hydroxyapatite (HA, $Ca_{10}(PO_4)_6(OH)_2$). In the fibers growing into the hydrogel, the (100) plane measured at 8.4 Å is parallel to the crystal growth direction. The measured (100) plane indexes range from 8.5 to 7.7 Å, as can be expected from the semicrystalline nature of the mineral particles.[17]

The mineralization patterns are determined by the characteristics of the electric-current-assisted diffusion process and the chemistry of the hydrogel scaffold. Ion migration at high concentration into the hydrogel promotes phase separation (a salt-out effect[18]). Spherical aqueous domains (∼0.5−1 μm in diameter) with a relatively large ionic content form inside the organic matrix as the polyacrylamide chains aggregate to open up the micrometer-sized pores while retaining the bulk gel structure (Figure 1d). Microphase separation results in the formation of aqueous domains with a very narrow size distribution whose diameter changes inversely with the hydrogel concentration (Supporting Information, Figure S-4). These domains play a role similar to that of the vesicles that mediate biomineralization.[2] Like the vesicles, the domains contain an aqueous solution with high ionic concentrations providing the right environment for mineral nucleation. The strong interaction between the amide group in the hydrogel and the Ca ions promotes the heterogeneous nucleation of nanocrystalline structures at the interface between these "artificial vesicles" formed by the phase separation process in the hydrogel.[19] The nanocrystals further assemble at the vesicle surface to form hollow microspheres (Figure 1c,d). Further growth occurs on both sides of the interface as the electric current continuously carries ions to the nucleation sites. Because of the different environments inside and outside of the synthetic vesicles (the crystals growing in the gel are confined by the polymer), the morphologies of the crystals growing into the hydrogel and toward the center of the vesicles are different (nanofiber and lamellar, respectively).

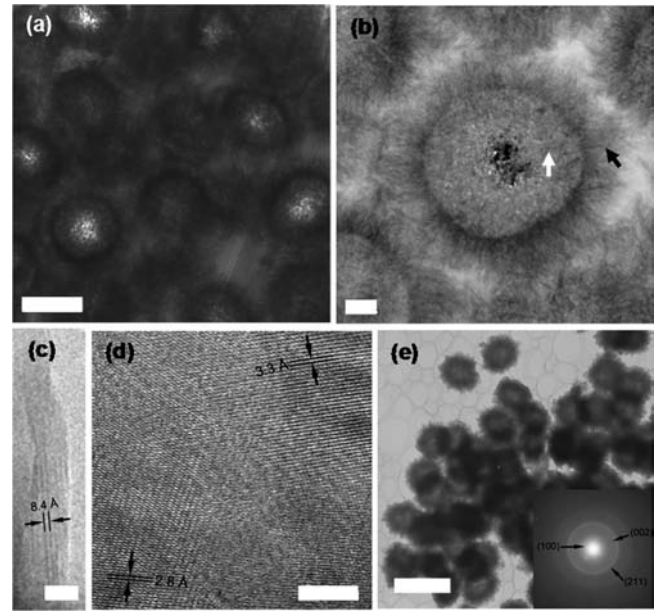

Figure 2. TEM images of the mineralized polyacrylamide hydrogel. FIB samples (a−d). (a) A low magnification image reveals a homogeneous distribution of HA mineral microspheres, ∼1 μm in diameter. (b) The dark field image of the microsphere shows its hollow structure. (c) The high resolution image of a mineral nanofiber growing in the organic matrix (black arrow in b) shows a mixture of amorphous and crystalline nanodomains. (d) The lamellar grains grown inside the microsphere (white arrow in b) also show a similar mixture of crystalline and amorphous nanodomains. (e) After stripping away the hydrogel of the bulk sample by oxygen plasma, hollow mineral aggregates with uniform size distribution can be observed. The corresponding electron diffraction pattern shown in the inset has the characteristic ring features of the HA (100) plane at 8.0 Å, (002) plane at 3.4 Å, and (211) plane at 2.9 Å with (211) being the strongest (Scale bar: (a) 1 μm; (b) 200 nm; (c) 5 nm; (d) 5 nm; (e) 2 μm).

The polyacrylamide network acts in two ways: first, it limits the size of the aqueous domains (the vesicles), and second, it provides nucleation sites for the formation of apatite.[20] In addition, the polymer also limits crystal growth inside the organic network resulting in the assembly of amorphous and crystalline (apatite) nanosized domains into a fiber arrangement. The critical role of the scaffold chemistry is illustrated by the mineralization behavior of the pHEMA gels. The hydroxyl groups on the pHEMA do not provide a binding place for the Ca ions.[15] Therefore brushite nucleates in the aqueous phase and grows uncontrollably into larger crystals that push the hydrogel away (Supporting Information, Figure S-2). This is not fully surprising as brushite is often found as a precursor for the formation of apatite in vitro although typically in more acidic conditions.[21,22] This result is consistent with previous experiments that have shown how the surface of pHEMA does not template the growth of calcium phosphate films during urea-based mineralization.[15]

The final mineral contents are ∼60% of the weight of the organics (Supporting Information, Figure S-5a). These large inorganic contents cannot be attained in bulk hydrogels using conventional methods. Other unique features of this process are

the formation of nanocrystals and their assembly into uniform hollow microspheres. The close packing of the spheres in the organic matrix provides the mechanical support needed to form a three-dimensionally connected microporous structure after removing the hydrogel through thermal treatment. The elimination of the polyacrylamide network using thermal treatments was monitored using differential thermal analysis and thermogravimetry (DTA-TG). Prior to the DTA, the hydrogel was dried at 37 °C for a week to remove water. After drying, the main crystalline phase is HA (Supporting Information, Figure S-5b). The broad diffraction peaks are in agreement with the semicrystalline and nanocrystalline nature observed in TEM experiments. The weight loss observed at temperatures up to 560 °C was due to the loss of residual water and decomposition of the hydrogel. The heat transition and weight loss observed above 600 °C are attributed to the phase transformation from apatite to β-tricalcium phosphate (β-TCP, $Ca_3(PO_4)_2$) as shown in the X-ray diffraction pattern (Supporting Information, Figure S-5b). The sharp and narrow diffraction peaks indicate the formation of a well-defined crystalline phase after firing. The microstructural evolution of the mineralized polyacrylamide hydrogel during heating is characterized first by the removal of the organic phase to leave the polycrystalline inorganic hollow spheres (Figure 3a) followed by their densification to form β-TCP microspheres with a very uniform particle size distribution (Figure 3b). The final step upon heating is the sintering of the tricalcium phosphate to create a microporous inorganic structure with a very uniformly distributed porosity, with a Brunauer−Emmett−Teller (BET) surface area of 0.68 m^2/g for the sintered structure (Figure 3c). The final pore sizes and specific surfaces may be controlled by manipulating the hydrogel concentration, the mineral content, and the sintering temperature (Supporting Information, Figure S-6). The detailed relationship is under investigation. This porous structure is much more homogeneous than the ones obtained after firing mixtures of synthetic nanosized HA particles with hydrogels. These exhibit a much more irregular microstructure due to the random aggregation of the mineral nanoparticles (Supporting Information, Figure S-7).

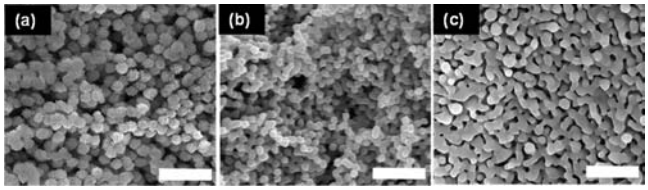

Figure 3. SEM micrographs of the mineralized polyacrylamide hydrogel heated at (a) 750, (b) 950, and (c) 1050 °C (Scale bar: 5 μm).

In conclusion, we have shown how current-assisted diffusion can be used to mimic vesicle-mediated mineralization in dense hydrogels. The mineralization technique and the chemistry of the organic matrix control the microstructure of the final material. Here we combine both aspects into a seamless process to develop hierarchical structures in which the organic and inorganic phases are integrated at the nanoscale while the mineral particles assemble into well-defined microscopic structures leading to high mineral concentrations. Some other parallels can be drawn between this process and bone development. The biomineralization of bone is believed to occur through the formation of intermediate phases, and there is some controversy regarding the first mineral phase to precipitate, either octacalcium phosphate (OCP) or an amorphous calcium phosphate (ACP).[23] It has been observed that DCDP and OCP can act as precursors to the formation of the apatitic phase in more acidic solutions *in vitro*.[21] In our system brushite nucleates when the matrix lacks specific sites to interact with the Ca ions. Still, the formation of DCDP seems to occur at higher pH than usually observed, suggesting that perhaps further research on the role played by the hydrogel in confining the nucleation sites inside the small aqueous domains is needed. Templating the mineral nucleation by functionalizing the polymer to promote a strong interaction with the Ca ions results in the formation of a nanostructured material with amorphous and poorly crystallized domains closer to what is observed in mature bone.[22] By controlling the microstructure and the mineral contents, we hope to develop hybrid materials with optimal mechanical and biological properties for the treatment of bone defects in a wide range of situations.

Acknowledgment. This work was supported by the National Institutes of Health (NIH) under Grant No. 5R01 DE015633. The FIB and TEM work was performed at the National Center for Electron Microscopy, Lawrence Berkeley National Laboratory, and was supported by the Office of Science, Office of Basic Energy Sciences, of the U.S. Department of Energy under Contract No. DE-AC02-05CH11231.

Supporting Information Available: Experimental procedures, Figures S-1, S-2, S-3, S-4, S-5, S-6, S-7. This material is available free of charge via the Internet at http://pubs.acs.org.

References

(1) Mayer, G. *Science* **2005**, *310*, 1144–1147.
(2) Mann, S. *Biomineralization: principles and concepts in bioinorganic materials chemistry*; Oxford University Press: Oxford, New York, 2001.
(3) Xu, A. W.; Ma, Y. R.; Colfen, H. *J. Mater. Chem.* **2007**, *17*, 415–449.
(4) Pouget, E.; Dujardin, E.; Cavalier, A.; Moreac, A.; Valery, C.; Marchi-Artzner, V.; Weiss, T.; Renault, A.; Paternostre, M.; Artzner, F. *Nat. Mater.* **2007**, *6*, 434–439.
(5) Hartgerink, J. D.; Beniash, E.; Stupp, S. I. *Science* **2001**, *294*, 1684–1688.
(6) Sanchez, C.; Arribart, H.; Guille, M. M. G. *Nat. Mater.* **2005**, *4*, 277–288.
(7) Peppas, N. A. *Hydrogels in Medicine and Pharmacy*; CRC Press: Boca Raton, FL, 1986.
(8) Barrera, D. A.; Zylstra, E.; Lansbury, P. T.; Langer, R. *J. Am. Chem. Soc.* **1993**, *115*, 11010–11011.
(9) Murphy, W. L.; Mooney, D. J. *J. Am. Chem. Soc.* **2002**, *124*, 1910–1917.
(10) Grassmann, O.; Lobmann, P. *Biomaterials* **2004**, *25*, 277–282.
(11) Taguchi, T.; Kishida, A.; Akashi, M. *Chem. Lett.* **1998**, 711–712.
(12) Hutchens, S. A.; Benson, R. S.; Evans, B. R.; O'Neill, H. M.; Rawn, C. J. *Biomaterials* **2006**, *27*, 4661–4670.
(13) Qu, H. B.; Xia, Z. M.; Knecht, D. A.; Wei, M. *J. Am. Ceram. Soc.* **2008**, *91*, 3211–3215.
(14) Watanabe, J.; Akashi, M. *Biomacromolecules* **2006**, *7*, 3008–3011.
(15) Song, J.; Saiz, E.; Bertozzi, C. R. *J. Am. Chem. Soc.* **2003**, *125*, 1236–1243.
(16) Masuyama, A.; Shindoh, A.; Ono, D.; Okahara, M. *J. Am. Oil Chem. Soc.* **1989**, *66*, 834–837.
(17) Sudarsan, K.; Young, R. A. *Acta Crystallogr. B* **1969**, *25*, 1534–1543.
(18) Liu, Q.; Hedberg, E. L.; Liu, Z. W.; Bahulekar, R.; Meszlenyi, R. K.; Mikos, A. G. *Biomaterials* **2000**, *21*, 2163–2169.
(19) Song, J.; Malathong, V.; Bertozzi, C. R. *J. Am. Chem. Soc.* **2005**, *127*, 3366–3372.
(20) Watanabe, J.; Akashi, M. *Biomacromolecules* **2007**, *8*, 2288–2293.
(21) Koutsoukos, P.; Amjad, Z.; Tomson, M. B.; Nancollas, G. H. *J. Am. Chem. Soc.* **1980**, *102*, 1553–1557.
(22) Dorozhkin, S. V.; Epple, M. *Angew. Chem., Int. Ed.* **2002**, *41*, 3130–3146.
(23) Brown, W. E. *Clin. Orthop. Relat. Res.* **1966**, *44*, 205–220.

JA903817Z